



Green synthesis of zinc oxide nanoparticles using flower extract of *Nyctanthes arbor-tristis* and their antifungal activity



Pragati Jamdagni*, Poonam Khatri, J.S. Rana

Department of Biotechnology, Deenbandhu Chhotu Ram University of Science and Technology, Murthal-131039, Sonapat, Haryana, India

Received 24 June 2016; accepted 4 October 2016
Available online 11 October 2016

KEYWORDS

Zinc oxide;
Phytosynthesis;
Electron microscopy;
Optical techniques;
Flower extract;
Antifungal activity

Abstract Biological reduction agents are being explored worldwide to minimize the effects of toxic chemicals used in nanoparticle fabrication. The present study states a green approach for the synthesis of zinc oxide nanoparticles employing aqueous flower extract of *Nyctanthes arbor-tristis*. Flower extract was used as the biological reduction agent for synthesizing zinc oxide nanoparticles from zinc acetate dihydrate. Synthesis conditions were optimized for maximal and narrow size range synthesis of zinc oxide nanoparticles. The resultant nanopowder was characterized using various analytical techniques, such as UV–Visible spectroscopy, Fourier Transform Infrared spectroscopy, X-ray diffraction, Dynamic Light Scattering and Transmission Electron Microscopy. The nanopowder was stored in dried form and was found to be stable after 4 months. The size range of nanoparticles obtained upon synthesis at optimum conditions was 12–32 nm as reported by TEM. X-ray diffraction studies confirmed the crystalline nature of the nanoparticles indicating particle size within the range provided by electron microscopy data. Nanoparticles were tested for their antifungal potential and were found to be active against all five tested phytopathogens with lowest MIC value recorded as 16 µg/mL. Hence, an easy and effective green approach for synthesis of zinc oxide nanoparticles, with efficient antifungal potential is reported in this study.

© 2016 The Authors. Production and hosting by Elsevier B.V. on behalf of King Saud University. This is an open access article under the CC BY-NC-ND license (<http://creativecommons.org/licenses/by-nc-nd/4.0/>).

1. Introduction

Nanoparticles are being synthesized globally owing to various exciting and unique properties, which facilitate their exploitation in completely unrelated fields, such as, nanodiagnostics (Jamdagni et al., 2016; Syed, 2014), nanomedicine (Bobo et al., 2016; Chen et al., 2016) and antimicrobials (Ahmed et al., 2016; Sirelkhatim et al., 2015) on one hand and luminescence (Diallo et al., 2016a,b; Sone et al., 2015; Thovhogi et al.,

* Corresponding author.

E-mail addresses: pragati_318@yahoo.co.in (P. Jamdagni), poonam-khatri2@gmail.com (P. Khatri), jsrana@outlook.com (J.S. Rana).

Peer review under responsibility of King Saud University.



Production and hosting by Elsevier

2016), photocatalytic potential (Diallo et al., 2016a,b; Eslami et al., 2016) and photodiode response (Thema et al., 2016) on the other. Zinc oxide nanoparticles (ZnO NPs), in particular, are environment friendly, offer easy fabrication and are non-toxic, biosafe and biocompatible making them an ideal candidate for biological applications (Mohammad et al., 2010; Rosi and Mirkin, 2005). Additionally, as per the US Food and Drug Administration, ZnO with other four zinc compounds have been listed as generally recognized as safe (GRAS) material (FDA, 2015). Various chemical methods have been proposed for the synthesis of ZnO NPs, such as reaction of zinc with alcohol, vapor transport, hydrothermal synthesis, precipitation method etc. However, these methods suffer various disadvantages due to the involvement of high temperature and pressure conditions and the use of toxic chemicals (Sabir et al., 2014). Green synthesis approaches are gaining interest circumventing the high costs and usage of toxic chemicals and harsh conditions for reduction and stabilization (Mason et al., 2012). In view of this, various metal and metal oxide nanoparticles have been successfully synthesized using biological methods (Husen and Siddiqi, 2014a, 2014b; Jeevanandam et al., 2016; Shanker et al., 2016; Singh et al., 2016), including some rare higher oxides such as Cr_2O_3 , Eu_2O_3 and Sm_2O_3 (Diallo et al., 2016a; Sone et al., 2016, 2015).

Recently, ZnO NPs have been used in food packaging materials and various matrices and methods for incorporation of ZnO into those matrices have been reported. ZnO is incorporated into the packaging matrix, free to interact with the food materials offering preservative effects (Espitia et al., 2012). Presently, ZnO NPs have found application in sunscreens, paints and coatings as they are transparent to visible light and offer high UV absorption (Franklin et al., 2007) and are also being used as an ingredient in antibacterial creams, ointments and lotions, self cleaning glass, ceramics and deodorants (Li et al., 2008). ZnO nanoparticles have been lately tested for their antimicrobial potential and seem to possess both antibacterial and antifungal potential. They are active against both Gram-positive and Gram-negative bacteria and also show considerable activity against more resistant bacterial spores (Azam et al., 2011). It was also observed that doping of ZnO NPs with other metals such as gold, silver, chromium etc. improved the antimicrobial activity of ZnO NPs (Jiménez et al., 2015; Shah et al., 2014). Also, inhibitory effects of ZnO nanosuspension are correlated with their size and concentration, with smaller particles offering better inhibitions in higher concentrations (Buzea et al., 2007; Padmavathy and Vijayaraghavan, 2008).

Nyctanthes, also known as Harsingar, is an important member of *Ayurveda*, the traditional Indian medicine science. It is blessed with a diverse spectrum of medicinal properties, such as being anti-helminthic, antimicrobial, antiviral, anti-leishmania, anti-allergic, anti-diabetic and anti-cancerous. It also serves as sedative and laxative agent, fights inflammation and has been widely used for the treatment of intermittent fevers and arthritis (Agrawal and Pal, 2013). *Nyctanthes* extracts have been reported to yield gold, silver and titanium dioxide nanoparticles (Das et al., 2011; Gogoi et al., 2015; Sundrarajan and Gowri, 2011).

Two majorly researched substrates for biosynthesis of ZnO NPs are zinc acetate (Davar et al., 2015; Hassan et al., 2015; Fatimah et al., 2016) and zinc nitrate (Diallo et al., 2015;

Sutradhar and Saha, 2016; Thema et al., 2015). This is, to the best of our knowledge, the first study reporting synthesis of zinc oxide nanoparticles using flower extract of *Nyctanthes arbor-tristis* and zinc acetate.

2. Material and methods

2.1. Materials

Zinc acetate dihydrate and all other chemicals were purchased from Thermo Fisher Scientific India Pvt. Ltd. (Mumbai). Flowers of *Nyctanthes arbor-tristis* were collected from the campus nursery of Deenbandhu Chhotu Ram University of Science and Technology, Murthal. Fungal phytopathogen slants were procured using commercial services of Indian Type Culture Collection, Indian Agricultural Research Institute, New Delhi.

2.2. Preparation of *Nyctanthes* flower extract

Fresh flowers of *Nyctanthes* were collected early in the morning and cleaned by washing several times with running water and subsequently with distilled water. Flowers were dried at room temperature in shade until all moisture was lost (12–14 days). Dried flowers were then ground to yield coarse powder, 10 gm of which was boiled in 100 mL of double distilled water for 15 min. The aqueous extract was then cooled, filtered using Whatman No.1 filter paper and stored at 4 °C for further use. Dried flowers were stored in an air tight container at room temperature for subsequent cycles of extract preparation.

2.3. Synthesis and optimization of synthesis parameters for zinc oxide nanoparticles

Zinc oxide nanoparticles were synthesized using zinc acetate dihydrate $\text{Zn}(\text{CH}_3\text{COO})_2 \cdot 2\text{H}_2\text{O}$ as described previously (Gnanasangeetha and Thambavani, 2013). Briefly, 0.01 M solution of zinc acetate was taken and flower extract was added. The pH of the mixture was maintained at 12 and the solution was stirred continuously for 2 h. A white precipitate resulted which was then dried at 60 °C overnight. Prior to drying, the precipitate was centrifuged at 15,000 rpm for 5 min and washed twice with sterile de-ionized water. Complete conversion to ZnO nanoparticles takes place during drying. However, the synthesis conditions were optimized for the current reaction by varying various parameters involved in synthesis. Various concentrations of zinc acetate, from .0025 M to .02 M, were used as substrates. Flower extract was added to 50 mL of zinc acetate solution in volumes ranging from 0.25 mL to 2 mL. The mixture was stirred continuously using a magnetic stirrer and was maintained at increasing pH values of 9, 10, 11, 12 and 13 using 2 M NaOH solution. Finally, reaction temperature was maintained at 60, 70, 80 and 90 °C. The same temperature at which synthesis was carried out was used for overnight drying of the precipitate obtained.

2.4. UV-Visible spectroscopy

For UV-Visible spectroscopy, the resultant nanopowder from each of the reactions was re-suspended in equal amount of

sterile de-ionized water and spectrum scans were performed using UV-Vis Spectrophotometer UV-3092 from Labindia Analytical Instruments Pvt. Ltd., in the wavelength range of 200–700 nm. The absorption values were re-plotted using OriginPro 8.

2.5. FT-IR spectroscopy

Fourier transform infrared (FT-IR) spectroscopy helps establish the identity of various phyto-chemical constituents involved in the reduction and stabilization of the nanoparticles. FT-IR spectrum for dried and powdered ZnO NPs was obtained using Perkin Elmer FT-IR Spectrophotometer Frontier using the technique of Attenuated Total Reflectance (ATR) in the range of 4000–500 cm^{-1} .

2.6. X-ray diffraction (XRD)

Washed and dried sample of ZnO NPs was used for XRD analysis using Ultima IV (Rigaku, Japan) at the wavelength of 1.5406 Å. XRD was performed in the 2θ range of 20–80 degrees at 40 kV and 40 mA with a divergence slit of 10 mm in $2\theta/\theta$ continuous scanning mode.

2.7. Dynamic Light Scattering (DLS)

The ZnO nanopowder was suspended in sterile de-ionized water and sonicated for 15 min prior to analysis. DLS of this suspension was then performed using Zetasizer Nano (DLS, Malvern Instruments, Worcestershire, UK). The Zetasizer is outfitted with a 633 nm wavelength He/Ne red laser and a detector fixed at 173° providing high sensitivity for size measurement. Hydrodynamic diameter and polydispersity index were measured as a function of time.

2.8. Transmission electron Microscopy (TEM)

For TEM, the ZnO nanopowder was suspended in sterile de-ionized water, sonicated for 15 min and diluted to yield slightly turbid suspension. The suspension was then coated onto a copper grid and allowed to dry. Morgagni 268D, FEI Electron Optics (USA) was used for TEM studies at an accelerating voltage of 200 kV. The results were visualized using Olympus siViewer.

2.9. Minimum inhibitory concentration (MIC) against fungal phyto pathogens

Synthesized ZnO NPs were tested for antifungal potential against *Alternaria alternata* (ITCC 6531), *Aspergillus niger* (ITCC 7122), *Botrytis cinerea* (ITCC 6192), *Fusarium oxysporum* (ITCC 55) and *Penicillium expansum* (ITCC 6755). The strains were maintained on potato dextrose agar at 28 °C. Spore suspensions were prepared using sterile normal saline solution by scraping and collecting conidia from 5 day old cultures. The suspension was then diluted to yield a spore count of 1×10^5 c.f.u./mL and used for MIC assays. MIC value was defined, primarily, based upon visual examination of fungal growth in serially diluted nanoparticle suspensions. 2 mL of media was poured in sterile tubes and 2 mL of ZnO NPs

(256 $\mu\text{g}/\text{mL}$) was then added in the first tube, which was then used for 2X dilution of consecutively numbered tubes. The tubes were then seeded with 100 μL of diluted spore suspension and incubated for 3 days at 28 °C. Absence of fungal growth was visually checked to define MIC values. All the experiments were performed in triplicates.

3. Results and Discussion

The pale white precipitate obtained was dried in hot air oven to yield zinc oxide nanopowder. The powder was re-suspended in deionized water to note the UV-Visible spectra showing an absorption peak at 369 nm (after 2 h) which remained stable after 3 h of reaction (Fig. 1a). The nanopowder synthesized at optimum conditions exhibited the sharpest peak of all the variations at 365 nm (Fig. 1b), was stored in dried form in centrifuge tubes and was found to be stable after 4 months of room temperature storage.

Increasing concentrations of zinc acetate were used to optimize the synthesis. An increase in absorption was observed when increasing the concentration of zinc acetate from .0025 M to .01 M accompanied by sharpening of peak. However, a further increase in concentration to .02 M resulted in decrease in absorbance as well as substantial broadening of peak. Hence, it was concluded that increasing the concentration of metal ions beyond a threshold value led to decrease in the synthesis of nanoparticles (Fig. 2a). On the same grounds, various concentrations of flower extract were explored for optimum synthesis. A steady improvement in the absorption and peak prominence was observed when increasing the extract volume from 0.25 mL to 1 mL. Maximum absorption was observed with 1 mL of flower extract in 50 mL of zinc acetate. Any increase or decrease in this volume led to decrease in the absorption values and hence, nanoparticle synthesis (Fig. 2b). Other major governing factors in green synthesis of nanoparticles are the pH and temperature of the reaction mixture. In this study, it was noted that increase in pH from 9 to 12 led to increase in the absorbance of the final product. While, an almost straight absorption line with no peak was observed at pH 9, spectrum at pH 12 and 13 showed characteristic absorption peak. However, absorbance and sharpness both were recorded to be better at pH 12 (Fig. 2c). Similarly, temperature is known to be one of the major effectors in the synthesis of nanoparticles. Spectra at 60 and 70 °C showed similar patterns with low and extremely broad peaks. While absorbance increased considerably at 80 °C, no prominent peak was observed. It was the synthesis at 90 °C that resulted in a remarkable increase in absorption coupled with a very sharp peak at 368 nm (Fig. 2d). No major peak shifts were observed during optimization reactions.

ZnO nanopowder obtained upon optimization was characterized using various analytical techniques to ascertain their size, shape and functionalization. First of all, to determine the role of flower extract in reduction and stabilization of the nanoparticles, FT-IR spectroscopy was performed. The FT-IR spectra resulted in various peaks at 3340.6, 3258.2, 2127.8, 1641.1, 1456.7, 1362.5, 1040, 1026.8, 746.25, 620.65 cm^{-1} (Fig. 3). The peaks at 3340.6 and 3258.2 correspond to H bonded OH stretch and N–H stretch (Awwad et al., 2013). Peak at 2127.8 corresponds to stretching vibrations of $\text{C} \equiv \text{C}$ stretch of alkynes (Spectroscopy Tutorial, 2016). The 1641.1

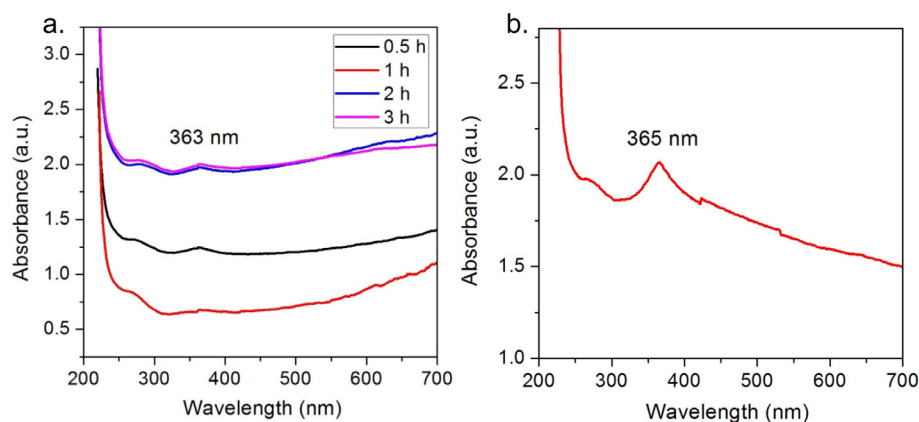


Figure 1 Synthesis of ZnO NPs, a. Time dependent, b. At optimum conditions.

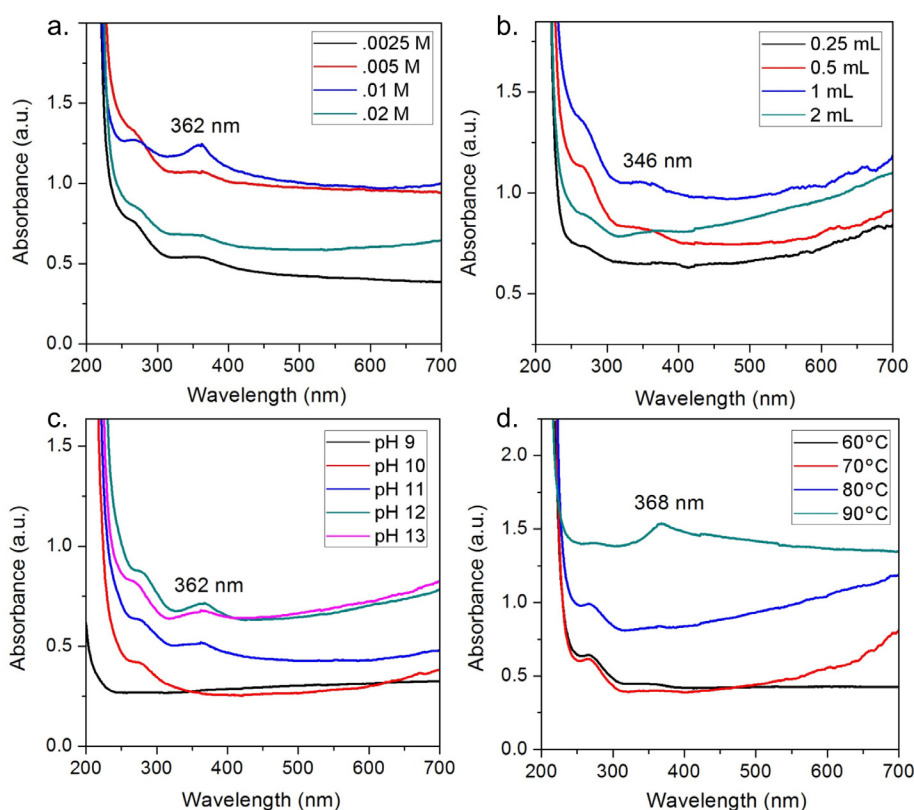


Figure 2 Optimization of synthesis parameters, a. Molarity of zinc acetate, b. Volume of flower extract, c. pH, d. Temperature.

peak results from the stretching bands of C=O functional groups (Rastogi and Arunachalam, 2011). The peak at 1456.7 refers to the amine —NH vibration stretch in protein amide linkages (Awwad et al., 2013). The 1362.5 peak results from aromatic amines and the two peaks at 1040 and 1026.8 result from C—N stretch of aliphatic amines. The 746.25 and 620.65 peaks correspond to alkanes and supposedly, C—H bend in alkynes, respectively (Das et al., 2011; Spectroscopy Tutorial, 2016). In the TEM images, a less intense layering is seen at the periphery of the nanoparticles (indicated by arrows in Fig. 4), which could relate to the capping of flower

components onto the resultant nanoparticles stating the role of biomolecules as reduction and capping agents.

Crystal lattice indices and particle size calculations were performed using the X-ray diffraction pattern of ZnO NPs (Fig. 5). Diffraction peaks were observed at 2θ values of 31.80° , 34.44° , 36.24° , 47.48° , 56.62° , 62.88° , 66.42° , 68.0° and 69.14° corresponding to lattice planes (100), (002), (101), (102), (110), (103), (200), (112) and (201) respectively. The peaks have been attributed to hexagonal phase of ZnO (JCPDS file: 36-1451) (Khoshhesab et al., 2011; Talam et al., 2012; Zhou et al., 2007).

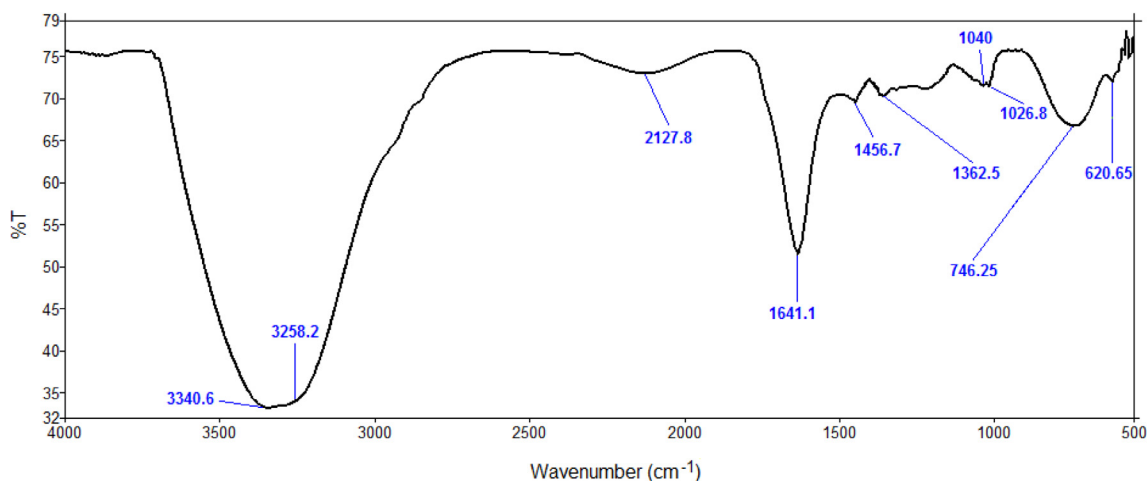


Figure 3 FT-IR Spectrogram of synthesized ZnO NPs.

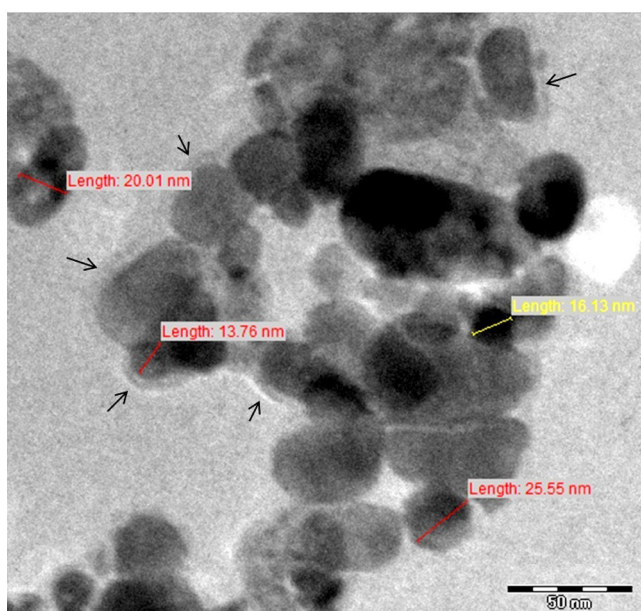


Figure 4 TEM images of ZnO NPs.

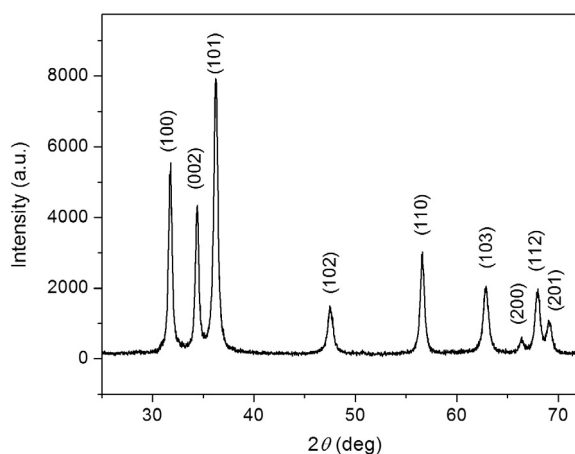


Figure 5 X-ray diffractogram of ZnO NPs.

Interplanar d -spacing was calculated using Bragg's Law equation (Table 1):

$$2d \sin \theta = n\lambda$$

where, θ is Bragg's angle of diffraction, λ is X-ray wavelength, i.e. 1.5406 Å and $n = 1$.

Further, particle size was calculated from the intense peak corresponding to (101) plane using Debye-Scherrer formula (Talam et al., 2012),

$$D = 0.89\lambda / \beta \cos \theta$$

where 0.89 = Scherrer's constant, λ = X-ray wavelength (1.5406 Å), β = FWHM (Full Width at Half Maximum) of the peak located at $2\theta = 36.24^\circ$ and θ = Bragg's angle of diffraction. The value of particle size was found to be 16.58 nm which falls within the size range of 12–32 nm reported by TEM.

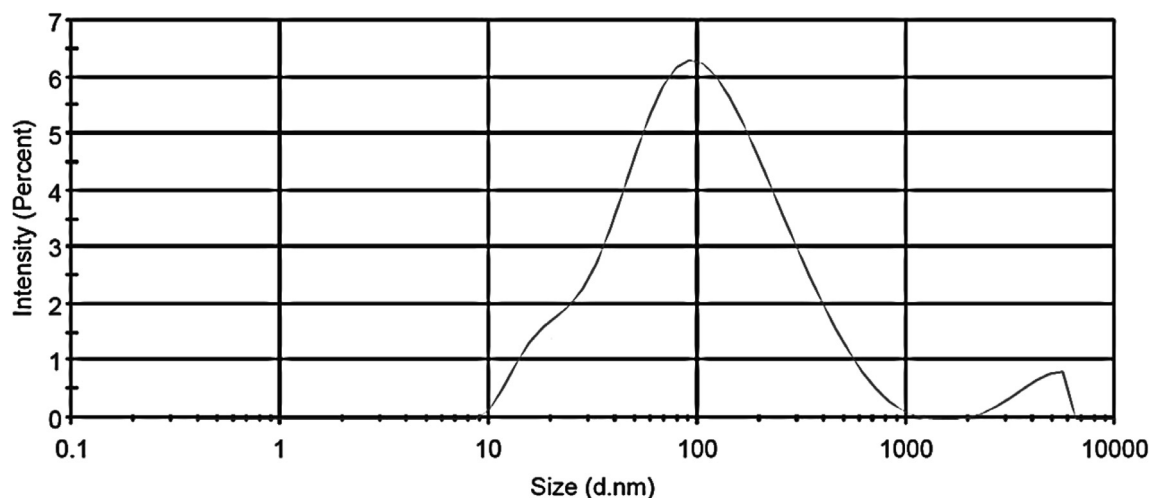
DLS is an emerging and vastly used technique for calculating the hydrodynamic diameter of nanoparticle suspensions based on Brownian movements exhibited by the particles. The average hydrodynamic diameter as calculated by DLS is 74.36 nm (Fig. 6) which is quite larger than the sizes reported by TEM and XRD.

This variation in NP sizes could be attributed to the poly-disperse nature of nanoparticles as indicated by the polydispersity index value of 0.488. Polydispersity is used to describe the degree of "non-uniformity" of a distribution and in the case of nanoparticle suspensions could be related to the occurrence of nanoparticles as aggregates or agglomerates, in turn causing variability in calculated particle size in comparison with the actual size of the particles. In TEM images, the presence of nanoparticle aggregates in the test suspension could be clearly seen, which further explains the larger hydrodynamic diameter given by DLS.

Phytopathogens destroy a major share of crop yields in the fields and also post harvest. Fungicides have been conventionally used for fungal control but their excessive use has fueled a new problem of generation of resistance against them (Leroch et al., 2011). Nanoparticles have emerged as a new class of antimicrobials and ZnO NPs have also recorded their presence as potential antimicrobial agents. Various interactions seem to be involved in ZnO NP mediated inhibitory effects on

Table 1 *d*-spacing calculations for ZnO NPs.

Peak 2θ	θ	$\sin \theta$	$d = n\lambda/2 \sin\theta$ (Å)	<i>d</i> (nm)	<i>hkl</i>
31.80	15.9	0.274	2.811	0.2811	100
34.44	17.22	0.296	2.602	0.2602	002
36.24	18.12	0.311	2.477	0.2477	101
47.48	23.74	0.403	1.911	0.1911	102
56.62	28.31	0.474	1.625	0.1625	110
62.88	31.44	0.522	1.476	0.1476	103
66.42	33.21	0.548	1.406	0.1406	200
68.00	34.00	0.559	1.378	0.1378	112
69.14	34.57	0.567	1.359	0.1359	201

**Figure 6** DLS results for ZnO NPs.

microbial cells. At first, as ZnO NPs come into contact with bacterial cells, they interact with the outer surface of the plasma membrane. This interaction disrupts the structure of plasma membrane and changes its permeability. Disruption of membrane structure and subsequent build up of ZnO NPs into the cytoplasm interfere with fundamental processes of cell growth (Sinha et al., 2011; Stoimenov et al., 2002; Zhang et al., 2007). Hydrogen peroxide has also been implemented as one of the major effectors in antibacterial effect mediated by ZnO NPs (Sawai et al., 1998). Additionally, ZnO NPs generate various other reactive oxygen species, such as hydroxyl radicals and singlet oxygen, which in turn stimulate cell death. Further, it was observed that while excitation of ZnO NPs with light improved the antimycotic effects, addition of ROS quencher histidine, on the contrary, led to complete suppression of inhibitory effects in yeast cells, emphasizing upon active involvement of ROS (Lipovsky et al., 2011).

Table 2 MIC values of ZnO NPs against target fungi.

Fungus	MIC ($\mu\text{g/mL}$)
<i>A. alternata</i>	64
<i>A. niger</i>	16
<i>B. cinerea</i>	128
<i>F. oxysporum</i>	64
<i>P. expansum</i>	128

In agreement with currently available reports, ZnO NPs synthesized using green method were found to possess good antifungal activity against all the tested fungi. Table 2 lists MIC values observed for various test fungi. *A. niger* was found to be most sensitive and showed lowest MIC value, while highest MIC value was observed for *B. cinerea* and *P. expansum*. Thus, nanoparticles can be used as potential antifungal agents and help overcome the hurdles in fungal disease management posed by development of resistance to conventional fungicides.

4. Conclusion

In the present study on “Green synthesis of zinc oxide nanoparticles using flower extract of *Nyctanthes arbor-tristis* and their antifungal activity”, zinc oxide nanoparticles were synthesized using aqueous flower extract of *Nyctanthes arbor-tristis*, a shrub commonly grown for ornamental purposes. Synthesis conditions were optimized and resultant nanopowder was characterized using UV-Visible spectroscopy, XRD, DLS and TEM. TEM images report individual particle size range of 12–32 nm and also revealed that the nanoparticles are present in the form of aggregates. In addition to morphological analysis, TEM analysis also establishes the role of a lesser intense capping layer on the NP surface. While studying the effect of nanoparticles for their antifungal potential, these showed good activity against 5 tested fungal

phytopathogens. It could be utilized for developing antifungal agents for commercial use in the field of agriculture. This study conclusively reports an eco-friendly approach for synthesis of zinc oxide nanoparticles. Such studies have potential for developing good fungicidal formulations having nanoparticles.

Acknowledgements

The author Pragati Jamdagni is thankful to Assured Opportunity for Research Careers (AORC), Department of Science and Technology (DST), Ministry of Science and Technology, New Delhi for awarding INSPIRE fellowship. All the authors are thankful to Sophisticated Analytical Instrument Facility (SAIF), AIIMS for providing TEM facility and Indian Agricultural Research Institute (IARI) for supply of fungal cultures.

References

- Agrawal, J., Pal, A., 2013. *Nyctanthes arbor-tristis* Linn—A critical ethnopharmacological review. *J. Ethnopharmacol.* 146 (3), 645–658.
- Ahmed, S., Ahmad, M., Swami, B.L., Ikram, S., 2016. A review on plants extract mediated synthesis of silver nanoparticles for antimicrobial applications: a green expertise. *J. Adv. Res.* 7 (1), 17–28.
- Awwad, A.M., Salem, N.M., Abdeen, A.O., 2013. Green synthesis of silver nanoparticles using carob leaf extract and its antibacterial activity. *Int. J. Ind. Chem.* 4, 29. <http://dx.doi.org/10.1186/2228-5547-4-29>.
- Azam, A., Ahmed, A.S., Oves, M., Khan, M.S., Habib, S.S., Memic, A., 2011. Antimicrobial activity of metal oxide nanoparticles against Gram-positive and Gram-negative bacteria: a comparative study. *Int. J. Nanomed.* 7, 6003–6009.
- Bobo, D., Robinson, K.J., Islam, J., Thurecht, K.J., Corrie, S.R., 2016. Nanoparticle-based medicines: a review of FDA-approved materials and clinical trials to date. *Pharm. Res.* 33 (10), 2373–2387. <http://dx.doi.org/10.1007/s11095-016-1958-5>.
- Buzea, C., Pacheco, I.L., Robbie, K., 2007. Nanomaterials and nanoparticles: sources and toxicity. *Biointerphases*, 2, pp. MR17–MR71.
- Chen, G., Roy, I., Yang, C., Prasad, P.N., 2016. Nanochemistry and nanomedicine for nanoparticle-based diagnostics and therapy. *Chem. Rev.* 116, 2826–2885. <http://dx.doi.org/10.1021/acs.chemrev.5b00148>.
- Das, R.K., Gogoi, N., Bora, U., 2011. Green synthesis of gold nanoparticles using *Nyctanthes arbor-tristis* flower extract. *Bioprocess Biosyst. Eng.* 34, 615–619.
- Davar, F., Majedi, A., Mirzaei, A., 2015. Green synthesis of ZnO nanoparticles and its application in the degradation of some dyes. *J. Am. Ceram. Soc.* 98, 1739–1746. <http://dx.doi.org/10.1111/jace.13467>.
- Diallo, A., Ngom, B.D., Park, E., Maaza, M., 2015. Green synthesis of ZnO nanoparticles by *Aspalathus linearis*: structural & optical properties. *J. Alloys Compd.* 646, 425–430.
- Diallo, A., Mothudi, B.M., Manikandan, E., Maaza, M., 2016a. Luminescent Eu₂O₃ nanocrystals by *Aspalathus linearis* extract: structural and optical properties. *J. Nanophotonics* 10, 26010. <http://dx.doi.org/10.1117/1.JNP.10.026010>.
- Diallo, A., Manikandan, E., Rajendran, V., Maaza, M., 2016b. Physical & enhanced photocatalytic properties of green synthesized SnO₂ nanoparticles via *Aspalathus linearis*. *J. Alloys Compd.* 681, 561–570. <http://dx.doi.org/10.1016/j.jallcom.2016.04.200>.
- Eslami, A., Amini, M.M., Yazdanbakhsh, A.R., Mohseni-Bandpei, A., Safari, A.A., Asadi, A., 2016. N, S co-doped TiO₂ nanoparticles and nanosheets in simulated solar light for photocatalytic degradation of non-steroidal anti-inflammatory drugs in water: a comparative study. *J. Chem. Technol. Biotechnol.* 91, 2693–2704.
- Espitia, P.J.P., Soares, N.F.F., Coimbra, J.S.R., de Andrade, N.J., Cruz, R.S., Medeiros, E.A.A., 2012. Zinc oxide nanoparticles: synthesis, antimicrobial activity and food packaging applications. *Food Bioprocess Technol.* 5, 1447–1464.
- Fatimah, I., Pradita, R.Y., Nurfalinda, A., 2016. Plant extract mediated of ZnO nanoparticles by using ethanol extract of *Mimosa pudica* leaves and coffee powder. *Procedia Eng.* 148, 43–48. <http://dx.doi.org/10.1016/j.proeng.2016.06.483>.
- FDA (Food and Drug Administration), Washington DC, USA, 2015. Select Committee on GRAS Substances (SCOGS) Opinion: Zinc Salts. < <http://www.fda.gov/Food/IngredientsPackagingLabeling/GRAS/SCOGS/ucm261041.htm> > (accessed 25.08.16).
- Franklin, N.M., Rogers, N.J., Apte, S.C., Batley, G.E., Gadd, G.E., Casey, P.S., 2007. Comparative toxicity of nanoparticulate ZnO, bulk ZnO, and ZnCl₂ to a freshwater microalga (*Pseudokirchneriella subcapitata*): the importance of particle solubility. *Environ. Sci. Technol.* 41 (24), 8484–8490.
- Gnanasangeetha, D., Thambavani, D.S., 2013. Biogenic production of zinc oxide nanoparticle using *Acalypha indica*. *J. Chem. Biol. Phys. Sci.* 4 (1), 238–246.
- Gogoi, N., Babu, P.J., Mahanta, C., Bora, U., 2015. Green synthesis and characterization of silver nanoparticles using alcoholic flower extract of *Nyctanthes arbor-tristis* and in vitro investigation of their antibacterial and cytotoxic activities. *Mater. Sci. Eng. C Mater. Biol. Appl.* 46, 463–469.
- Hassan, S.S.M., El-Azab, W.I.M., Ali, H.R., Mansour, M.S.M., 2015. Green synthesis and characterization of ZnO nanoparticles for photocatalytic degradation of anthracene. *Adv. Nat. Sci. Nanosci. Nanotechnol.* 6, 045012. <http://dx.doi.org/10.1088/2043-6262/6/4/045012>.
- Husen, A., Siddiqi, K.S., 2014a. Plants and microbes assisted selenium nanoparticles: characterization and application. *J. Nanobiotechnol.* 12, 28. <http://dx.doi.org/10.1186/s12951-014-0028-6>.
- Husen, A., Siddiqi, K.S., 2014b. Phytosynthesis of nanoparticles: concept, controversy and application. *Nanoscale Res. Lett.* 9, 229. <http://dx.doi.org/10.1186/1556-276X-9-229>.
- Jamdagni, P., Khatri, P., Rana, J.S., 2016. Nanoparticles based DNA conjugates for detection of pathogenic microorganisms. *Int. Nano Lett.* 6, 139–146. <http://dx.doi.org/10.1007/s40089-015-0177-0>.
- Jeevanandam, J., Chan, Y.S., Danquah, M.K., 2016. Biosynthesis of metal and metal oxide nanoparticles. *ChemBioEng Rev.* 3, 55–67. <http://dx.doi.org/10.1002/cben.201500018>.
- Jiménez, A.B.P., Aguilar, C.A.H., Ramos, J.M.V., Thangarasu, P., 2015. Synergistic antibacterial activity of nanohybrid materials ZnO–Ag and ZnO–Au: synthesis, characterization, and comparative analysis of undoped and doped ZnO nanoparticles. *Aust. J. Chem.* 68, 288–297.
- Khoshshesab, Z.M., Sarfaraz, M., Asadabad, M.A., 2011. Preparation of ZnO nanostructures by chemical precipitation method. *Synth. React. Inorg. Met.-Org. Nano-Met. Chem.* 41 (7), 814–819.
- Leroch, M., Kretschmer, M., Hahn, M., 2011. Fungicide resistance phenotypes of *Botrytis cinerea* isolates from commercial vineyards in South West Germany. *J. Phytopathol.* 159, 63–65.
- Li, Q., Mahendra, S., Lyon, D.Y., Brunet, L., Liga, M.V., Li, D., Alvarez, P.J., 2008. Antimicrobial nanomaterials for water disinfection and microbial control: potential applications and implications. *Water Res.* 42 (18), 4591–4602.
- Lipovsky, A., Nitzan, Y., Gedanken, A., Lubart, R., 2011. Antifungal activity of ZnO nanoparticles—the role of ROS mediated cell injury. *Nanotechnology* 22, 105101. <http://dx.doi.org/10.1088/0957-4484/22/10/105101>.
- Mason, C., Vivekanandhan, S., Misra, M., Mohanty, A.K., 2012. Switchgrass (*Panicum virgatum*) extract mediated green synthesis of silver nanoparticles. *World J. Nano Sci. Eng.* 2, 47–52.

- Mohammad, V., Umar, A., Hahn, Y.B., 2010. ZnO nanoparticles: growth, properties, and applications. In: Umar, A., Hahn, Y.B. (Eds.), *Metal Oxide Nanostructures and Their Applications*. American Scientific Publishers, USA, pp. 1–36.
- Padmavathy, N., Vijayaraghavan, R., 2008. Enhanced bioactivity of ZnO nanoparticles—an antimicrobial study. *Sci. Technol. Adv. Mat.* 9, 1–7.
- Rastogi, L., Arunachalam, J., 2011. Sunlight based irradiation strategy for rapid green synthesis of highly stable silver nanoparticles using aqueous garlic (*Allium sativum*) extract and their antibacterial potential. *Mater. Chem. Phys.* 129, 558–563.
- Rosi, N.L., Mirkin, C.A., 2005. Nanostructures in biodiagnostics. *Chem. Rev.* 105 (4), 1547–1562.
- Sabir, S., Arshad, M., Chaudhari, S.K., 2014. Zinc oxide nanoparticles for revolutionizing agriculture: synthesis and applications. *Sci. World J.* 2014, 925494. <http://dx.doi.org/10.1155/2014/925494>.
- Sawai, J., Shoji, S., Igarashi, H., Hashimoto, A., Kokugan, T., Shimizu, M., Kojima, H., 1998. Hydrogen peroxide as an antibacterial factor in zinc oxide powder slurry. *J. Ferment. Bioeng.* 86, 521–522. [http://dx.doi.org/10.1016/S0922-338X\(98\)80165-7](http://dx.doi.org/10.1016/S0922-338X(98)80165-7).
- Shah, A.H., Manikandan, E., Basheer Ahamed, M., Ahmad Mir, D., Ahmad Mir, S., 2014. Antibacterial and Blue shift investigations in sol-gel synthesized $\text{Cr}_x\text{Zn}_{1-x}\text{O}$ Nanostructures. *J. Lumin.* 145, 944–950. <http://dx.doi.org/10.1016/j.jlumin.2013.09.023>.
- Shanker, U., Jassal, V., Rani, M., Kaith, B.S., 2016. Towards green synthesis of nanoparticles : from bio-assisted sources to benign solvents. A review. *Int. J. Environ. Anal. Chem.* 96 (9), 801–835. <http://dx.doi.org/10.1080/03067319.2016.1209663>.
- Singh, P., Kim, Y.J., Zhang, D., Yang, D.C., 2016. Biological synthesis of nanoparticles from plants and microorganisms. *Trends Biotechnol.* 34 (7), 588–599. <http://dx.doi.org/10.1016/j.tibtech.2016.02.006>.
- Sinha, R., Karan, R., Sinha, A., Khare, S.K., 2011. Interaction and nanotoxic effect of ZnO and Ag nanoparticles on mesophilic and halophilic bacterial cells. *Bioresour. Technol.* 102, 1516–1520. <http://dx.doi.org/10.1016/j.biortech.2010.07.117>.
- Sirelkhatim, A., Mahmud, S., Seeni, A., Kaus, N.H.M., Ann, L.C., Bakhori, S.K.M., Hasan, H., Mohamad, D., 2015. Review on zinc oxide nanoparticles: antibacterial activity and toxicity mechanism. *Nano-Micro Lett.* 7, 219–242. <http://dx.doi.org/10.1007/s40820-015-0040-x>.
- Sone, B.T., Manikandan, E., Gurib-Fakim, A., Maaza, M., 2015. Sm_2O_3 nanoparticles green synthesis via *Callistemon viminalis* extract. *J. Alloys Compd.* 650, 357–362. <http://dx.doi.org/10.1016/j.jallcom.2015.07.272>.
- Sone, B.T., Manikandan, E., Gurib-Fakim, A., Maaza, M., 2016. Single-phase $\alpha\text{-Cr}_2\text{O}_3$ nanoparticles' green synthesis using *Callistemon viminalis* red flower extract. *Green Chem. Lett. Rev.* 9, 85–90. <http://dx.doi.org/10.1080/17518253.2016.1151083>.
- Spectroscopy Tutorial. Chemistry and Biochemistry Department. University of Colorado, Boulder. <<http://orgchem.colorado.edu/Spectroscopy/specttutor/irchart.pdf>> (accessed 01.01.16).
- Stoimenov, P.K., Klinger, R.L., Marchin, G.L., Klabunde, K.J., 2002. Metal oxide nanoparticles as bactericidal agents. *Langmuir* 18 (17), 6679–6686.
- Sundrarajan, M., Gowri, S., 2011. Green synthesis of titanium dioxide nanoparticles by *Nyctanthes arbor-tristis* leaves extract. *Chalco-genide Lett.* 8, 447–451.
- Sutradhar, P., Saha, A., 2016. Green synthesis of zinc oxide nanoparticles using tomato (*Lycopersicon esculentum*) extract and its photovoltaic application. *J. Exp. Nanosci.* 11, 314–327. <http://dx.doi.org/10.1080/17458080.2015.1059504>.
- Syed, M.A., 2014. Advances in nanodiagnostic techniques for microbial agents. *Biosens. Bioelectron.* 51, 391–400.
- Talam, S., Karumuri, S.R., Gunnam, N., 2012. Synthesis, characterization, and spectroscopic properties of ZnO nanoparticles. *ISRN Nanotechnol.* 2012, 372505. <http://dx.doi.org/10.5402/2012/372505>.
- Thema, F.T., Manikandan, E., Dhlamini, M.S., Maaza, M., 2015. Green synthesis of ZnO nanoparticles via *Agathosma betulina* natural extract. *Mater. Lett.* 161, 124–127. <http://dx.doi.org/10.1016/j.matlet.2015.08.052>.
- Thema, F.T., Manikandan, E., Gurib-Fakim, A., Maaza, M., 2016. Single phase Bunsenite NiO nanoparticles green synthesis by *Agathosma betulina* natural extract. *J. Alloys Compd.* 657, 655–661. <http://dx.doi.org/10.1016/j.jallcom.2015.09.227>.
- Thovhogi, N., Park, E., Manikandan, E., Maaza, M., Gurib-Fakim, A., 2016. Physical properties of CdO nanoparticles synthesized by green chemistry via *Hibiscus Sabdariffa* flower extract. *J. Alloys Compd.* 655, 314–320. <http://dx.doi.org/10.1016/j.jallcom.2015.09.063>.
- Zhang, L., Jiang, Y., Ding, Y., Povey, M., York, D., 2007. Investigation into the antibacterial behaviour of suspensions of ZnO nanoparticles (ZnO nanofluids). *J. Nanoparticle Res.* 9, 479–489. <http://dx.doi.org/10.1007/s11051-006-9150-1>.
- Zhou, J., Zhao, F., Wang, Y., Zhang, Y., Yang, L., 2007. Size controlled synthesis of ZnO nanoparticles and their photoluminescence properties. *J. Lumin.* 122–123 (1–2), 195–197.